TECHNOLOGY for FUTURE and AGEING PIPELINES
29 – 31 March 2022 Gent | Belgium

STRESS STATE EFFECT ON HYDROGEN EMBRITTLEMENT OF HIGH-STRENGTH STEELS

Wenqi Liu[1], Jiaojiao Wu[1], Eric Fangnon[1], Evgenii Malitckii[1], Pedro Vilaça[1], Junhe Lian[1]

[1] Department of Mechanical Engineering, Aalto University, 02150 Espoo, Finland

ABSTRACT: This study investigates the hydrogen effect on the behavior of high-strength steels under different stress states. The research is focused on tensile testing with in-situ hydrogen charging. The hydrogen charging is performed electrochemically. Hydrogen uptake, trapping, and diffusivity are studied by the thermal desorption spectroscopy method. Based on the finite element simulation, the pre-designed notches on the dog-bone tensile test specimen geometry are introduced to achieve the constant stress state until fracture initiation. The focused stress states are the central-hole tension, notched-dog-bone tension, and shear. A constant loading speed is applied during the testing. Additional tensile testing without hydrogen charging is conducted as the reference. The stress state coupling hydrogen influence is characterized by the response maximum force and fracture displacement. It is proved that the sensitivity of hydrogen embrittlement on high-strength steels is strongly stress-state dependent.

1. INTRODUCTION

With the increased demand for clean energy and requirements of the excellent combination of high strength and good ductility, the high-strength steel sheets are more and more focused on in terms of their mechanical behavior under hydrogen environment continues to pose an essential bottleneck for their utilization in industrial field (Depover et al., 2019); (Loidl et al., 2011). Hydrogen atoms can ingress into the metal lattice and accumulate in higher stressed zones and interact and trap in metal lattice imperfections, i.e. voids, dislocations, grain boundaries, precipitates, second-phase particles, etc. (Pundt et al., 2006). This process will result in the formation of hydrogen-enriched positions, degrade the material mechanical behavior and ultimately, reduce the lifetime of the component, which is well known as hydrogen embrittlement (HE). Several mechanisms, such as hydrogen-enhanced localized plasticity (HELP) (Beachem, 1972); (Birnbaum et al., 1994), hydrogen-enhanced decohesion (HEDE) (Troiano, 2016), hydrogen-enhanced strain-induced vacancy formation (HESIV) (Nagumo, 2004), and several others, have been proposed to explain the HE phenomenon. In addition, due to the dual- or multi-phase structure with fine grain size, the complex microstructure contained in most high-strength steels would increase the complication in the HE-related mechanisms. Several studies are focusing on the HE phenomenon in high-strength steels. Mallick et al. (2021) has studied microstructural influence on the hydrogen diffusivity behavior of dual-phase (DP) and complex-phase (CP) steels with tensile strength around 800-1000 MPa using the electrochemical method. There is a finding that the lower total H

concentration along with a higher fraction of H was present in the stronger traps in steels. Hwang et al. (2021) investigated the influence of constituent phases on hydrogen-induced mechanical degradation in two high-strength steel sheets with tensile strength over 1180 MPa. It was proved that hydrogen-induced loss in tensile strength of the CP steel is not significant as it is in the elongation. With a loss of less than 5% in tensile strength for all charging conditions in the investigated CP steel, the loss in total elongation can reach 70% at a charging time of 48 h. Drexler et al. (2021) has studied the hydrogen susceptibility of cold-formed and heat-treated DP and CP steel sheets with tensile strength larger than 1200 MPa. There is a very strong effect of the microstructure on the resistivity on hydrogen embrittlement in high-strength steels. Futhermore, Bal et al. (2020) has studied the effect of hydrogen on the mechanical response and fracture locus of commercial twinning induced plasticity steels by hybrid experiments and numerical methods. The deterioration in the mechanical response due to hydrogen was observed regardless of the sample geometry and hydrogen changed the fracture mode from ductile to brittle. Currently, research concerning the stress state's effect on the tensile property and damage mechanism of advanced high-strength CP steels is rare, which is significant to be investigated. In the current project, we are focusing on a high-strength steel, CP1000 with tensile strength around 1000 MPa, which is composed of bainitic, austenitic, martensite, etc. Understanding the mechanical performance in the hydrogen environment could be further extended to other high-strength steels.

In this study, the electromechanical charging method is applied to study the hydrogen diffusivity behavior of CP1000 steel. Several typical geometries of tensile specimens are designed to cover different stress states in uniaxial tensile loading conditions. In-situ hydrogen charging uniaxial tensile testing is carried out for CP1000 to study the potential hydrogen embrittlement mechanism. To quantitatively evaluate the damage and fracture property of CP1000 with or without a hydrogen environment, numerical simulation is operated to find the crack initiation strain and compare.

2. MATERIAL AND EXPERIMENTAL PROGRAM

A high-strength CP1000 steel sheet with a thickness of 1 mm is investigated in the study. It consists of martensite, bainite, ferrite, and small amounts of retained austenite and cementite. The average grain size is smaller than 5 μm. The most important alloying elements in CP1000 are 0.12 wt% C, 0.26 wt% Si, 2.2 wt% Mn, 0.23 wt% Cr, etc.

To study the stress state's effect on CP1000 steel considering the hydrogen environment, uniaxial tensile tests have been applied along the RD direction with or without in-situ electrochemical hydrogen charging. The same loading condition and specimen geometries were used for all tensile testing with or without hydrogen. The testing was performed at room temperature with a Zwick/Roell Z030 screw-driven tensile testing machine, which has a maximum load capacity of 30 kN. All the sheet specimens have a total length of 250 mm, width of 15 mm, and thickness of 1mm. Except for the standard smooth dog-bone (SDB) specimens, the geometries of fractured tensile specimens were designed according to Liu et al. (2019) to involve the varying stress states. The chosen geometry notches are an in-plane central hole with a diameter of 4 mm for central-hole specimens (CHD4), two symmetrical in-plane edge notches with a radius of 40 mm for notched-dog-bone specimens (NDBR40), two rounded eccentric positioned in-plane notches with a radius of 1mm for shear specimens (SH). **Figure 1** (a) shows the tensile sample geometry with detailed features. The quasi-static loading condition was employed for all specimens: a strain rate of 10^{-4} s^{-1} for SDB and loading velocity of 0.15 mm/min for all fractured tensile specimens. All specimens were cut by electrical discharge machining then ground to P1200 sandpaper and cleaned by ethanol.

To perform the hydrogen tensile testing, the optimal charging parameters need to be determined first. The chemical solution is a weak acid prepared by 2 L aqueous solution, 60 g NaCl and 2 g NH_4SCN. One independent Gamry Interface 1010 potentiostat was used to control the electrochemical reaction. In this study, the H+ was reduced galvanostatically with the static potential of -1.41 V. The potential represented an overcurrent of -10 mA, to make sure the charging procedure is mild and quick. According to the thermal desorption spectroscopy measurement of the total hydrogen content in the specimen, it was concluded that the investigated CP1000 steel with a thickness of 1 mm could reach a saturated state by charging 30 minutes in the electrochemical solution. For the tensile testing with hydrogen, the additional electrochemical charging cell was installed on the Zwick machine, as shown in **Figure 1** (b). The specimens were immersed in the charging chamber and pre-charged for 30 minutes before the loading started. At least three parallel tests were conducted for each loading condition.

(a)

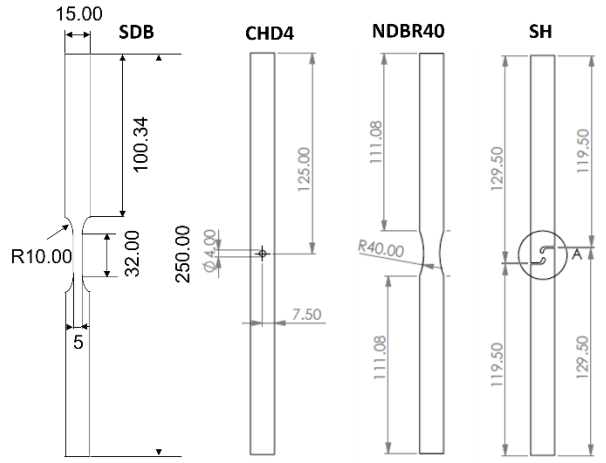

(b)

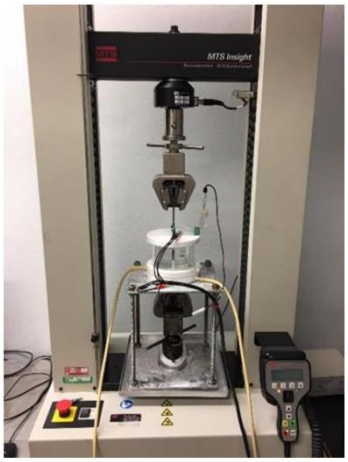

Figure 1. Uniaxial tensile test setup. (a) Geometry of tensile specimens (unit: mm). (b) In-situ hydrogen charging device coupled with test machine (Fangnon et al., 2021).

3. NUMERICAL SIMULATION SET UP

According to the geometries of the fractured tensile testing, the finite element (FE) models were built up with the Abaqus/Explicit software. Considering the realistic boundary conditions in the mechanical testing with in-situ hydrogen charging, the full in-plane geometry was set up. The regions with 25 mm length away from the top and bottom edges were set as the clamping areas with constraint boundary conditions, which were the clamping regions in the testing. During the deformation, the bottom clamping region was fully constrained, while the movement of the top clamping region was prevented in five freedom degrees, i.e. except the tension direction. The required displacement along the tension direction was applied to the nodes on the top edges with a constant velocity. In addition, to save the simulation time, the 1/2 models with the symmetry on the thickness direction were chosen for all investigated geometries. Hence, the nodes on the z-symmetrical plane are restricted to moving in the z-direction. To minimize the mesh effect among varying geometries, a consistent mesh method was employed. The regular 3D brick elements with reduced integration (C3D8R) were chosen in all models. The critical deformation regions were meshed with fine 3D elements with the size of 0.1 mm × 0.1 mm × 0.1 mm, with the transition regions, the elements size gradually changed to 2 mm × 2 mm × 0.25 mm for the rest parts of the model. The fully meshed FE models with the in-plane zoom-in for the critical deformation zones are shown in **Figure 2**.

Based on the tensile testing flow curve without hydrogen charging, the combined Voce–Swift law in equation 1 was used to extrapolate the flow curve until the true plastic strain of 3, which was employed as the hardening las in the Mises simulation.

$$\bar{\sigma}_y = 0.8 \times \left(922.8 + 162.0 \times (1 - e^{-52.86 \times \bar{\varepsilon}_p})\right) + 0.2 \times \left(1254 \times \left(5.13 \times 10^{-5} + \bar{\varepsilon}_p\right)^{0.051}\right) \quad (1)$$

Where $\bar{\sigma}_y$ is the flow stress and $\bar{\varepsilon}_p$ is the equivalent plastic strain (PEEQ). The experimental and calibrated flow curve are plotted in **Figure 3**. It is noted that the calibrated parameters in the hardening law were also validated according to the comparations of the force–displacement responses of the different geometries between the experiments and simulation. From the simulation, the loading history of the critical elements until the crack initiation moment in each geometry can be calculated. The stress triaxiality and Lode angle parameter are used to characterize the stress states according to Bai et al. (2008) and Lian et al. (2013) etc.

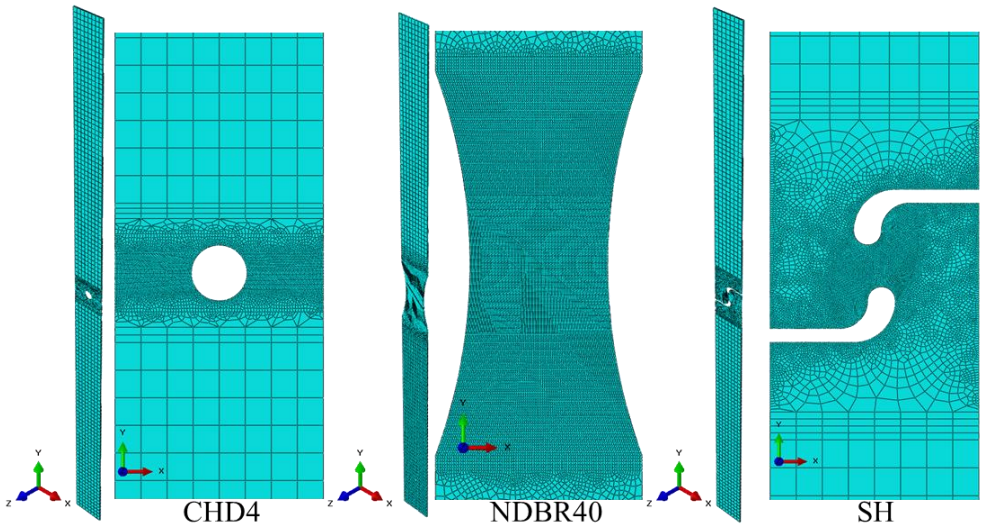

Figure 2. FE model setup of fractured tensile testing samples.

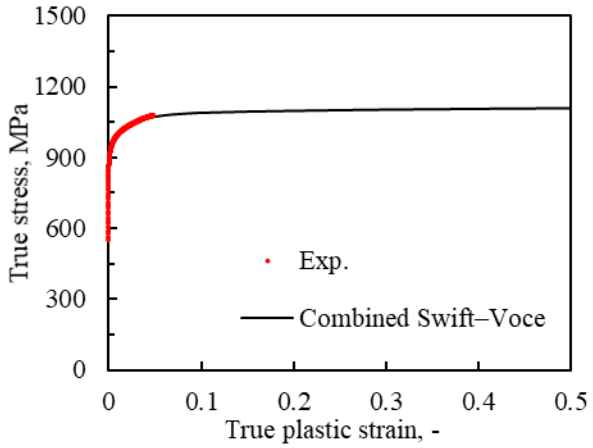

Figure 3. Flow curve extrapolation based on the combined Swift–Voce law.

4. RESULTS AND DISCUSSION

4.1 Tensile property

The results of uniaxial tensile tests are presented in **Figure 4** with solid lines for tests without hydrogen and dot lines for in-situ hydrogen-charging tests, including the engineering stress–strain curves of the SDB specimens and force–displacement curves of featured stress-states specimens. It should be noted that as the gauge length displacement cannot be directly measured during the in-situ hydrogen-charging tensile tests, the recorded displacement of the whole specimen from the experiments needs to be corrected based on the elastic part prediction from simulation. As shown in **Figure 4**, the SDB specimens display an obvious reduction of ductility while the ultimate tensile strength (UTS) has no big difference between original and hydrogen charged samples. The distinctive reduction of ductility in the hydrogen environment can also be observed for all featured stress states specimens. However, the quantity of ductility reduction is different from each other. With the lowest stress triaxiality and Lode angle parameter, the shear specimen performs the lowest strength and the extended uniform plastic deformation range in the testing without hydrogen. However, hydrogen brings the earliest force drop and localization behavior in SH. The hydrogen environment promotes the necking behavior of SH specimens with a reduction in the uniform displacement of 67.8% compared to the one without the hydrogen effect. Regarding NDBR40 specimens, they hold the highest stress triaxiality and intermediate Lode angle parameter showing the lowest ductility reduction, whose fracture displacement is reduced 14.3% by hydrogen. CHD4 specimens hold the highest Lode angle parameter and intermediate stress triaxiality. The

reduction of fracture displacement is about 22.4%, so they have the intermediate ductility reduction. Based on the current results, it seems that the lower stress triaxiality would bring a higher ductility reduction by hydrogen. Besides, the hydrogen also affects the UTS of CP1000 steel. The results display that, SH and CHD4 show a smaller decrease of UTS in the hydrogen environment, but NDBR40 has the same. According to the HELP mechanism, the presence of hydrogen in the lattice structure of steel as the solid solution would enhance the dislocation motion ability, therefore, the plastic deformation occurring in a localized region would increase adjacent to the fracture surface (Birnbaum et al., 1994). HELP would accelerate the crack initiation procedure and reduce the ductility of the CP1000 steel, as shown in **Figure 4**. Further study should be considered to investigate the hydrogen diffusivity and trapping behavior of CP1000 under varying stress states. The observation on fractography and microstructure-related damage mechanism would be involved to reveal the mechanisms of stress state effect on HE behavior.

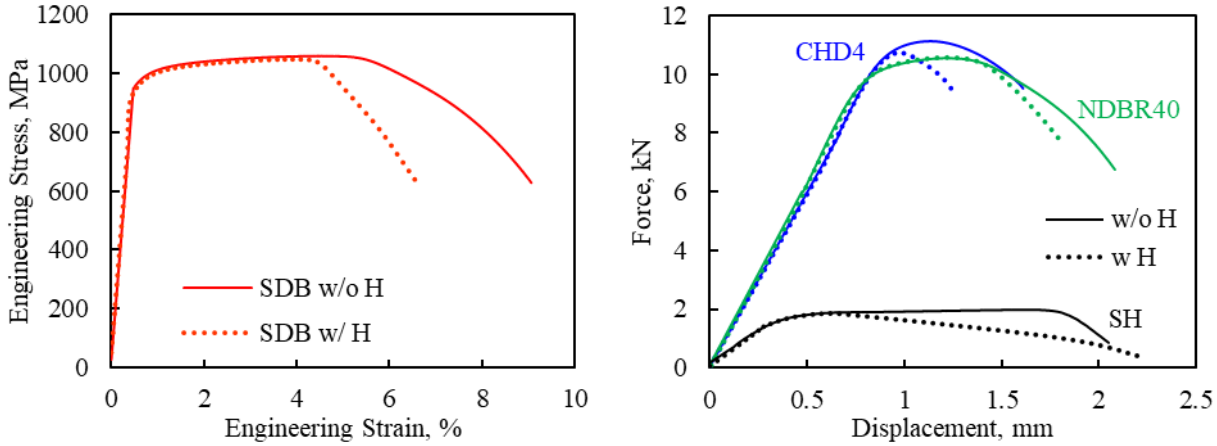

Figure 4. Results of CP1000 steel in uniaxial tensile testing with or without hydrogen charging.

4.2 Fracture strain

For all tensile testing with or without hydrogen charging, the crack initiation moment is defined as the sudden force drop occurrence on the force–displacement curves. The critical element is regarded as the maximum equivalent plastic strain position in the FE models, which is the central element of NDB specimens, central element close to the hole edge of CH specimens, and the central element with maximum PEEQ value in the shear region on the symmetry plane of SH specimens. With the same geometries, hardening law, and boundary conditions in the simulation, the loading history of the critical elements of each geometry is also the same for testing with or without hydrogen charging, as shown in **Figure 5**. It can be seen that both stress triaxiality and Lode angle parameter of SH are close to zero during the whole loading history. The obviously non-proportional loading path is found in CH and NDB specimens, especially for the without hydrogen charging specimens due to the postponed crack initiation strain. Without hydrogen charging, the investigated CP1000 has a good crack resistance, especially, the crack initiation strain of CHD4 and NDBR40 specimens is nearly 2.0. The shear stress state brings the lowest crack initial strain, which is the same of both testing w/ or w/o hydrogen. Furthermore, hydrogen results in the distinctly smaller crack initial strain for all specimens, which is consistent with the shortened ductility in the tensile testing. However, varying stress states are accompanied by the different hydrogen effects. The crack initial strain of CH is higher than the NDB specimens without hydrogen charging, while it dropped approximately 76% with hydrogen charging. Meanwhile, the reduction of crack initial strain caused by hydrogen embrittlement in NDBR40 is only 31%. Therefore, the influence of stress states on the hydrogen embrittlement cannot be ignored. The translation motion of the fracture locus only based on the smooth uniaxial tensile testing or limited fracture tests is not accurate to predict the metal fracture behavior with HE. The calibration of the stress-state informed HE fracture locus is necessary. For the force drop at the maximum point and post-necking stage, a softer hardening law might be considered for the specimens under a hydrogen environment. To qualify the influence of stress states on HE sensitivity, more stress state conditions should be involved to calibrate the fracture loci with and without hydrogen with the improved modeling performance.

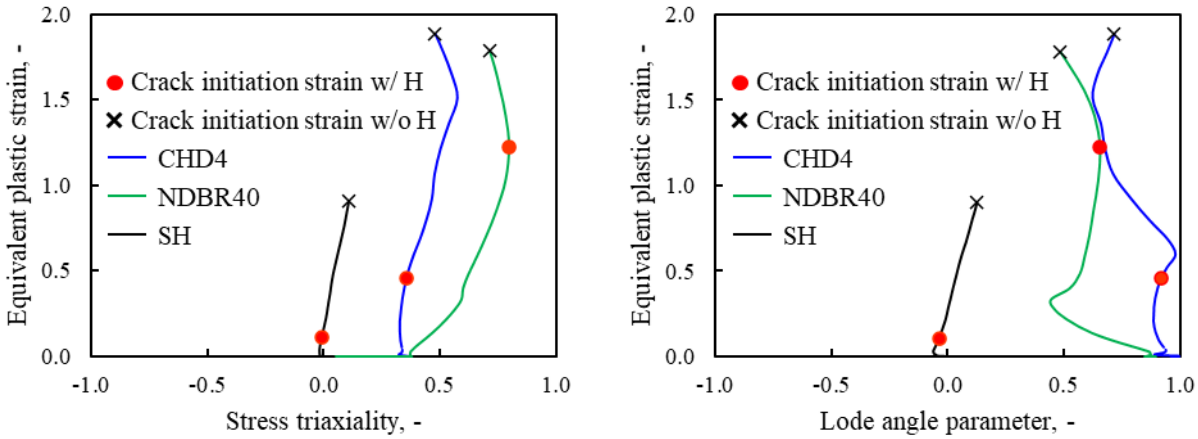

Figure 5 Loading paths of the critical elements of CHD4, NDBR6, and SH specimens.

5. REMARKS

The uniaxial tensile testing on a CP1000 steel sheet with and without the hydrogen environment was performed in this study to investigate the influence of stress state on hydrogen embrittlement. It can be concluded that the sensitivity of hydrogen is affected by varying stress states. The microstructure-related damage and fracture mechanisms of stress state effect on hydrogen embrittlement including the hydrogen diffusivity and trapping behavior should be investigated in further study.

6. REFERENCES

Bai, Y., Wierzbicki, T., (2008). "A new model of metal plasticity and fracture with pressure and Lode dependence", *International Journal of Plasticity*, 24, pp. 1071-1096.

Bal, B., et al., (2020). "Effect of hydrogen on fracture locus of Fe–16Mn–0.6C–2.15Al TWIP steel", *International Journal of Hydrogen Energy*, 45, pp. 34227-34240.

Beachem, C.D., (1972). "A new model for hydrogen-assisted cracking (hydrogen "embrittlement")", *Metallurgical and Materials Transactions B*, 3, pp. 441-455.

Birnbaum, H.K., Sofronis, P., (1994). "Hydrogen-enhanced localized plasticity—a mechanism for hydrogen-related fracture", *Materials Science and Engineering: A*, 176, pp. 191-202.

Depover, T., et al., (2019). "Evaluation of the hydrogen embrittlement susceptibility in DP steel under static and dynamic tensile conditions", *International Journal of Impact Engineering*, 123, pp. 118-125.

Drexler, A., et al., (2021). "On the local evaluation of the hydrogen susceptibility of cold-formed and heat treated advanced high strength steel (AHSS) sheets", *Materials Science and Engineering: A*, 800, pp. 140276.

Fangnon, E., et al., (2021). "Determination of Critical Hydrogen Concentration and Its Effect on Mechanical Performance of 2200 MPa and 600 HBW Martensitic Ultra-High-Strength Steel", *Metals*, 11, pp. 984.

Hwang, A.I., et al., (2021). "Influence of Microstructure Constituents on the Hydrogen-Induced Mechanical Degradation in Ultra-High Strength Sheet Steels", *Metals and Materials International*, 27, pp. 3959-3967.

Lian, J., et al., (2013). "A hybrid approach for modelling of plasticity and failure behaviour of advanced high-strength steel sheets", *International Journal of Damage Mechanics*, 22, pp. 188-218.

Liu, W., et al., (2019). "Damage mechanism analysis of a high-strength dual-phase steel sheet with optimized fracture samples for various stress states and loading rates", *Engineering Failure Analysis*, 106, pp. 104138.

Loidl, M., et al., (2011). "Characterization of hydrogen embrittlement in automotive advanced high strength steels", *Materialwissenschaft und Werkstofftechnik*, 42, pp. 1105-1110.

Mallick, D., et al., (2021). "Study of Diffusible Behavior of Hydrogen in First Generation Advanced High Strength Steels", *Metals*, 11, pp. 782.

Nagumo, M., (2004). "Hydrogen related failure of steels – a new aspect", *Materials Science and Technology*, 20, pp. 940-950.

Pundt, A., Kirchheim, R., (2006). "HYDROGEN IN METALS: Microstructural Aspects", *Annual Review of Materials Research*, 36, pp. 555-608.

Troiano, A.R., (2016). "The Role of Hydrogen and Other Interstitials in the Mechanical Behavior of Metals", *Metallography, Microstructure, and Analysis*, 5, pp. 557-569.